Development and Characterization of Nanoemulsion-based Buccal Films of Atorvastatin Calcium for Enhancement of Hypolipidemic Effect

Fatma Bakr[1], Moetaza M. Soliman[2*], Hassan M. Elsabbagh[1]

[1] Department of Pharmaceutics, Faculty of Pharmacy, Mansoura University, Egypt

[2] Department of Clinical Pharmacy and Pharmacy Practice, Faculty of Pharmacy, Mansoura University, Egypt

* Corresponding Author: Email address: moetaza@mans.edu.eg

Postal address: Faculty of Pharmacy, Mansoura University, Elgomhoria Street, Mansoura, Eldakahlia, Egypt.

Abstract

Objectives: Atorvastatin calcium (ATC) is widely used to treat hyperlipidemia but its effectiveness is limited by its low oral bioavailability. The aim of this study was to formulate and evaluate mucoadhesive buccal films containing ATC-loaded nanoemulsion (NE) in an attempt to enhance ATC hypolipidemic effectiveness.

Methods: Based on various parameters, including ATC saturation solubility, NE mean droplet size, clarity, thermodynamic stability, and flowability, the optimum NE components were selected which included 10% oleic acid as oil phase, 50% tween 20: ethanol at different ratios as surfactant co-surfactant mixture (SCmix) and 40% water. ATC mucoadhesive buccal films were prepared using hydroxypropyl methylcellulose mixed with the selected optimum ATC-loaded NE by solvent casting technique. Prepared films were subjected to various evaluations including physicochemical characteristics, mucoadhesive properties, ex vivo drug release and finally subjected to in vivo study to evaluate the effectiveness in treating rabbits with diet-induced hyperlipidemia.

Results: NE-based film and control film showed acceptable physical characteristics without significant difference in the mucoadhesive properties. NE-based film was more effective in enhancing the penetration of ATC than the control film through chicken pouch membrane by non Fickian mechanism. The in vivo study revealed that both blood analysis and histopathological examination proved the superior effectiveness of NE-based film in reduction of cholesterol level in rabbits with hyperlipidemia over the control film.

Conclusion: The formulated NE-based mucoadhesive buccal films were successful in enhancement of hypolipidemic benefits of ATC, in tested rabbits, in comparison to the control film through improving the solubility and bioavailability of ATC.

Keywords: nanoemulsion, mucoadhesive, HPMC, hypercholesterolemia, rabbits.

1- Introduction

Nanoemulsions (NEs) are translucent dispersions of two immiscible liquids (oil and water) that are stabilized by an interfacial coating of surfactant molecules with droplet sizes ranging from 20 to 200 nm (Jaiswal, Dudhe, and Sharma 2015). Many researchers have been interested in these formulations because of their simplicity of manufacture, scale-up and stability (Debnath, Satayanarayana, and Kumar 2011).

NEs offer a promising method for improving the oral bioavailability of poorly soluble drugs (Yen et al. 2018). They are claimed to be free of destabilizing phenomena such as sedimentation, creaming, coagulation and flocculation due to their small droplet size (Azmi et al. 2019). Innovative drug delivery systems, such as the mucoadhesive buccal systems, can improve the drug bioavailability and efficiency. Drugs, which show low bioavailability via the oral route due to hepatic first-pass metabolism, their bioavailability, can be enhanced when used in the form of mucoadhesive buccal delivery systems to avoid hepatic first-pass metabolism (Kumar et al. 2019).

Atorvastatin calcium (ATC) is a cholesterol -lowering drug that belongs to hydroxymethyl glutaryl-coenzyme A reductase inhibitors or statins. ATC is used to minimize the risk of stroke, heart attack, and other heart problems in people who have type-2 diabetes, coronary heart disease, or other risk factors (Poli 2007). ATC has a low-solubility (Rodde et al. 2014) and a low oral bioavailability (14 %) due to significant hepatic first-pass metabolism (Lennernäs 2003).

The goal of this study was to improve the solubility of ATC by creating a thermodynamically stable and dilutable NEs formulation of ATC with the lowest possible surfactant concentration. The study also aimed to load the produced NEs into mucoadhesive buccal films, characterize the produced films, and assess the hypolipidemic effect of ATC.

2-Material and Methods

2.1-Material

ATC was kindly gifted from Amoun pharmaceutical company, Cairo, Egypt. Hydroxypropyl methylcellulose (HPMC k100), tween 20, and oleic acid were supplied from LANXESS Energizing Chemistry, Cologne, Germany. Tween 80, polyethylene glycol (PG), and absolute ethanol were supplied from Adwic - El-Nasr Pharmaceutical Chemicals, Qaliubiya, Egypt. BRIJ-35 (nonionic surfactant) was purchased from Loba Chemie PVT.LTD., Mumbai, India. Cholesterol was purchased from ADVENTCHEMBIO PVT.LTD, Navi Mumbai, India. Semipermeable cellulose membrane (molecular weight cut off of 12,000–14,000) was obtained from Spectrum Medical Industries Inc., Los Angeles, USA. Formalin was supplied from Research-Lab Fine Chem Industries, Mumbai, India. All other materials were of fine analytical grade.

2.2-Preparation of NEs

2.2.1-Selection of oil phase, surfactant and co-surfactant

The ATC saturation solubility was measured in different oils (oleic acid, olive, sunflower, and soya bean oil), different surfactants (tween 20, tween 80, and brij 35), and different co-surfactants (propylene glycol and absolute ethanol). The solubility was measured using thermostatically controlled agitating water bath (Grant

Zagazig J. Pharm. Sci. Dec, 2021
Vol. 30, Issue 2, pp. 23- 40

ISSN 1110-5089
ISSN (on-line) 2356_9786

Instrument, Cambridge Ltd., UK). In 8-mL stoppered vials, excess amount of ATC was dissolved in 2 mL of each of the chosen oils, surfactants, or co-surfactants. The samples were mixed using a vortex mixer (Stuart Scientific, United Kingdom) at 1200 pm and maintained at 37°C for 24 hours to reach equilibrium. The equilibrated samples were then removed from the shaker, centrifuged and diluted with methanol. The supernatant was filtered using a 0.45 µm filter. UV spectrophotometry at a maximum wavelength of 246 nm was used to measure ATC concentration in each sample (Abu-Huwaij et al. 2019).

2.2.2-Pseudoternary phase diagrams of NEs

According to the results of the solubility tests, an oil phase, surfactant, and a co-surfactant of oleic acid, tween 20, and ethanol, respectively, were chosen for the preparation of pseudo-ternary systems. Double distilled water was utilized as aqueous phase.

Six combinations of the surfactant (tween 20) and co-surfactant (ethanol) were prepared by mixing at different ratios (3:1, 2:1, 1:1, 1:2, 1:3, and 1:4 w/w). The six surfactant co-surfactant mixtures (SCmix) were assessed visually for miscibility, transparency (clarity) and for ease of flow. SCmix combinations that were immiscible, turbid, or had poor flowability were excluded from any further analysis.

The prepared SCmix combinations were vortexed violently for half a minute. The oil phase (oleic acid) and SCmix were blended in different proportions (1:9, 2:8, 3:7, 4:6, 5:5, 6:4, 7:3, 8:2, and 9:1, w/w respectively). Using the aqueous titration method and a vortex mixer, aqueous phase (distilled water) was added gradually, mixed for 5 minutes, equilibrating the system between each addition. The mixture was visually inspected for transparency and clarity after each addition of each aliquot of aqueous phase. The phase diagrams were used to depict the physical condition of the NEs, with three axis denoting an aqueous phase, oil phase, and SCmix. A NE region was plotted for each phase diagram, and the larger the area, the greater the self nanoemulsifying efficiency (Ramadan et al. 2013). Within the NEs region of the constructed pseudo-ternary phase diagram a ratio was selected to determine the amounts of oil: water: SCmix to be used in the preparation of the NEs.

The selected formulations from the NEs area of constructed phase diagrams to prepare the NEs should allow the integration of ATC dose in the oil phase easily at minimum amount of oil with the minimum concentration of SCmix.

2.2.3-Preparation of ATC-loaded NEs

NEs of (o/w) type were made by combining 10% w/w oleic acid, 40% w/w water, and 50% w/w SCmix. To make a clear combination, ATC was dissolved at a consistent concentration in the oil phase. With continual vortexing, SCmix of all specified systems was introduced to the oil/ATC mixture. Water was added to make ATC-loaded NEs by using the aqueous titration method (Jain et al. 2013). Between each addition of water, the samples were vortexed for 15 minutes at 2500 rpm and allowed to equilibrate .

2.3-Characterization of ATC-loaded NEs
2.3.1-Thermodynamic stability studies

Drug-loaded NEs were tested using centrifugation, heating/cooling cycles, and freeze/thaw cycles. The NEs were first centrifuged for 15 min at 3500 rpm. If there was no phase separation present, NEs were exposed to six heating (45 °C) and cooling (4 °C) cycles. The duration of each cycle was 48 hours to ensure that they remained

Zagazig J. Pharm. Sci. Dec, 2021
Vol. 30, Issue 2, pp. 23- 40

ISSN 1110-5089
ISSN (on-line) 2356_9786

clear. Three freeze (- 21 °C) and thaw (25 °C) cycles were performed on NEs for 48 hours per cycle to see if they remained transparent (Shafiq et al. 2007).

2.3.2- Droplet size analysis

The average droplet size, Zeta potential, and polydispersity index (PDI) of NEs were measured using Malvern Zetasizer Nanoseries, (Malvern Instruments Limited, UK). At a temperature of 25°C and a 90° angle, light scattering was measured. The samples were diluted 100 times in distilled water before being inserted directly into the module. For each formulation, three replicate analyses were performed, with data provided as mean ± SD (Ali et al. 2014).

2.3.3-Transmission electron microscopy

The structure and morphology of the chosen NEs were determined using a transmission electron microscopy (JEOL JEM-2100, JEOL Ltd, Tokyo, Japan). The NEs was diluted 100 times using distilled water, stained for 30 seconds with 2% (w/v) phosphotungstic acid, and deposited on a carbon-coated grid to be studied after drying.

2.4-Preparation of mucoadhesive buccal films

2.4.1-Calculation of the dose of ATC in the film

ATC is available as 10, 20, 40, and 80 mg conventional tablets (Singh et al. 2008). Due to hepatic metabolism, the quantity reaching the systemic circulation from oral tablets is only 14% (oral bioavailability). The proposed buccal route offers a systemic bioavailability that is likely to approach unity (100%) because of the direct access of the drug to the systemic circulation, through the internal jugular vein, and bypassing the hepatic first pass metabolism. Therefore ATC dose was reduced to 1.4, 2.8, 5.6 or 11.2 mg in the mucoadhesive buccal films (Hassan et al. 2009).

2.4.2-Preparation of ATC control and NE-based films

Nanoemulsions NE1, NE2, NE3 and NE4 were used to prepare F1, F2, F3, and F4 mucoadhesive buccal films, respectively.

ATC-loaded NE-based mucoadhesive buccal films were formulated using a solvent casting technique by the addition of the chosen ATC-loaded NEs containing 71.48 mg ATC to 0.5 g HPMC followed by mixing using a magnetic stirrer for 2 hrs until a homogenous and regular mixture was achieved. The amount of ATC was calculated based on the surface area of the used petri dish. Then the mixture was poured in 25.5 cm^2 petri dish. This mixture was dried for 48 hours with a constant air flow at room temperature until the film is formed. The dried films were elastic enough to be peeled easily from the glass petri dishes and cut by a sharp cutter into 2×2 cm^2 squares each containing 11.2 mg ATC (Abu-Huwaij et al. 2019). The films were wrapped in aluminum foil and stored in a desiccator for further evaluation.

For comparison, a control mucoadhesive buccal film (F0) was prepared by the same method. The control film was loaded with ATC but without the nanoemulsion base. An amount of 71.48 mg of ATC was dissolved in ethanol and added to 0.5 g HPMC aqueous blend and then a plasticizer (propylene glycol) was added, and kept for stirring for 2 hrs. Care was taken during stirring to avoid air bubble entrapment. After uniform mixing, the solution was casted into 25.5 cm^2 petri dish and dried for 48 hours with a constant air flow at room temperature. The dried formed films were cut into 2×2 cm^2 squares each containing 11.2 mg ATC, and stored in a desiccator for further evaluation.

2.5-Spectral and thermal analyses

ATC alone, physical mixture prepared by mixing equal amounts of ATC and HPMC, ATC-loaded NE-based film, HPMC alone, plain film (not loaded with ATC), and control film were analyzed by Fourier Transform Infrared (FTIR) spectrophotometer (Nicolet iS10, Thermo Fisher Scientific, U.S.A.). Samples were scanned over a range of wave number from $500\ cm^{-1}$ to $4000\ cm^{-1}$. The FTIR spectra of different samples were compared to that of pure ATC (Nair et al. 2020).

The thermal characteristics of ATC alone, physical mixture of ATC and HPMC, ATC-loaded NE-based film, HPMC alone, plain film, and control film were studied using Perkin-Elmer, differential scanning calorimeter (DSC 6000, Waltham, MA, USA). In a liquid nitrogen atmosphere flowing at a rate of 20 ml/minute, the thermograms of the samples were recorded. Each sample's thermal response was studied at a rate of $10^{o}C/min$ throughout a temperature range from room temperature to $350\ ^{o}C$ (Salehi and Boddohi 2017).

2.6- Evaluation of physicochemical properties of films

2.6.1-Thickness

Thicknesses of both ATC-loaded NE-based film and the ATC control film were measured three times from different places and the mean ($\pm$SD) values were determined using Micrometer screw gage (Mitutoyo, Japan) (Semalty, Semalty, and Nautiyal 2010).

2.6.2-Weight variation

Ten randomly chosen films were weighed and the mean weights ($\pm$SD) were calculated using Electric Balance (Zakiady Mechanikr Precyzyjnej Merrwag Gdansk, Poland) (Semalty, Semalty, and Nautiyal 2010).

2.6.3-Folding endurance

Folding endurance was determined by the number of times the film was folded in the same axis repeatedly until it tears (El-Maghraby and Abdelzaher 2015).

2.6.4-Drug content uniformity

The ATC content in the prepared films was measured by dissolving them in 10 mL methanol and stirring overnight at room temperature. Three samples were analyzed for drug content. The solution was filtered from the film residues then suitably diluted and the amount of drug in each film was measured spectrophotometrically at 246 nm after adequate dilution (El-Maghraby and Abdelzaher 2015).

2.6.5- Moisture content

Each selected film was accurately weighed and stored in desiccators packed with anhydrous calcium chloride for three days. The film was then removed from the desiccator and reweighed. The percentage of moisture content was calculated using a formula "% Moisture content = (Initial weight- Final weight)/ Initial weight $\times$100" (Augusthy et al. 2014).

2.6.6-Swelling index

In a clean petri dish containing 50 mL of pH 6.8 phosphate buffer, the pre weighted films were placed and the increase in the weight of the films was noted every 5 minutes until there is no increase in the weight. The swelling index (SI) was computed using the formula "SI = (film weight at time t – film weight at time zero) / film weight at time zero" (El-Maghraby and Abdelzaher 2015).

2.6.7-Surface pH

Using a combined glass electrode pH-meter (Beckman Instrument Fullerton, CA 92634, Germany) the surface pH of the prepared mucoadhesive buccal films ($2\times2\ cm^{2}$) was tested. The films were allowed to swell in 1 ml of distilled water for 2 hours at room

Zagazig J. Pharm. Sci. Dec, 2021
Vol. 30, Issue 2, pp. 23- 40

ISSN 1110-5089
ISSN (on-line) 2356_9786

temperature before the surface pH was measured (Ammanage et al. 2020).

2.6.8- Surface Morphology

Scanning electron microscope (JSM 6150 - JEOL, Japan) was used to examine the surface texture and distribution of ingredients of ATC-loaded buccal films. After being mounted to a sample holder with double sided adhesive tapes, samples were inserted in the apparatus, examined, and pictured at suitable magnification (Nair et al. 2020).

2.6.9-Ex-vivo mucoadhesion time

Modified USP disintegration apparatus (Erweka Apparatus, Germany) was used in this procedure. The tested mucoadhesive ATC-loaded film was placed with gentle pressing on the mucosal side of a piece of chicken pouch membrane which was glued to a glass slide fixed to the apparatus (Mohamed, Haider, and Ali 2011). The glass slide was allowed to move up and down in the media (300 mL phosphate buffer pH 6.8). The mucoadhesion time was computed by the time needed for complete detachment of the film (Desai and Pramod Kumar 2004).

2.6.10- Mucoadhesive strength

To measure the mucoadhesive strength of ATC-loaded buccal films, the modified physical balance method was used (Pendekal and Tegginamat 2012). Briefly, the tested mucoadhesive ATC-loaded film was placed on the mucosal side of a piece of chicken pouch membrane which was secured in one of 2 balanced pans filled with phosphate buffer pH 6.8. Water drops were added gradually in the other pan until the film was dislodged from the membrane. The weight (grams) of the additional water needed to separate the film was used to calculate mucoadhesive strength which was then multiplied by 981 to calculate the force of adhesion (Dyne) (Giradkar et al. 2010).

2.6.11- Ex vivo drug permeation studies

The drug release from the prepared ATC-loaded NEs-based and control mucoadhesive buccal films was studied using vertical Franz diffusion cell (Shailaja et al. 2012) (3 cm in diameter) placed in shaking incubator and maintained at 37 ± 0.5 °C. A fresh piece of chicken pouch membrane was washed well and any adipose tissue was removed. The membrane was mounted between the diffusion cells' donor and receptor chambers. The receptor chamber was filled with phosphate buffer (pH 6.8) containing a solubilizer (30% methanol). Stirring at 50 rpm was maintained to mimic buccal condition. In a donor cell containing 2 mL of buffer, the film was placed on the mucosal side of the membrane. A sample of 3 ml from the receptor compartment was withdrawn hourly for up to 8 hours. To keep the sink condition, an equivalent volume of fresh medium was carefully introduced to the receiver compartment. The aliquots were filtered via a Millipore filter and ATC concentration was measured spectrophotometerically at 246 nm.

Variety of mathematical models, including zero-order, first-order, Higuchi, and Korsmeyer–Peppas equations were used to study the kinetic analysis of ex vivo ATC permeation through chicken pouch membrane.

2.7-In vivo study and histopathological evaluation

Institutional ethical approval was obtained from the Faculty of Pharmacy-Mansoura University ethical committee before running the in vivo study utilizing rabbits.

Experiment was done on twelve Newzeland white male rabbits weighting 2.0-2.5 kg. Before beginning the experiment, blood samples were taken from the rabbit's ear vein. The blood samples were centrifuged at

Zagazig J. Pharm. Sci. Dec, 2021
Vol. 30, Issue 2, pp. 23- 40

ISSN 1110-5089
ISSN (on-line) 2356_9786

5000 rpm for 10 min to separate plasma. The collected plasma samples were analyzed for various biochemical parameters like total cholesterol, high density lipoprotein (HDL), and triglyceride level, using commercially available diagnostic kits (HUMAN Gesellschaft für Biochemica und Diagnostica, Germany).

Rabbits were then fed high fat diet meals containing normal chow mixed with 0.3% cholesterol and egg yolk as a source of cholesterol (Sumbul and Ahmed 2012) for 4 weeks to induce hyperlipidemia (Chen, Wang, and Wu 2020). Blood samples were taken again and analyzed to ensure the occurrence of hyperlipidemia.

At this stage animals were allocated to three groups the first one did not receive any formulation, second group received the control ATC-loaded films (F0) and the third group received ATC-loaded NEs-based mucoadhesive buccal film (F2) with daily dose of 5mg/kg for 14 days (Rashid et al. 2002). Each rabbit was placed under anesthesia using isoflurane inhalation to allow the application of the tested film formulations to the rabbit's buccal mucosa (Holpuch et al. 2012). Blood samples were collected after 2 weeks of treatment from each rabbit and the plasma were separated by centrifugation at 5000 rpm for 10 minutes and analyzed for various biochemical parameters.

The control rabbits were sacrificed after induction of hyperlipidemia. Other animals were sacrificed after two weeks of treatment. The heart and the liver of all sacrificed animals were excised and examined histologically. Isolated heart and liver tissues were fixed at room temperature in 10% formalin. Haematoxylin and eosin dye were used to stain the sectioned tissues which were then examined, under light microscope, for any histological changes.

2.8 Statistical analysis

The results were presented as mean $\pm$ SD for continuous variables or as percentages. Unpaired T-test was used to compare results between two groups while the paired T-test was used to compare the response in the same group before and after receiving the treatment. P values < 0.05 were interpreted as significant differences.

3-Results and discussion

In this study, mucoadhesive buccal films (F1 to F4) containing ATC-loaded NEs were prepared with a main purpose of enhancing the hypolipidimic effect of ATC. Table 1 shows the composition of the prepared films. First the components of the NEs were selected. Then the appropriate NEs were loaded with ATC (NE 1-4). Finally the NE-based mucoadhesive buccal films were prepared. A control mucoadhesive buccal film containing ATC without NE was also prepared (F0).

3.1- Selection of oil phase, surfactant and co-surfactant

According to the data presented in Table 2, ATC showed better solubility in oleic acid than that in soybean, olive and sunflower oil. Hence, oleic acid was chosen as the oil phase for the preparation of NEs. The nonionic surfactant tween 20 was used in formulating NEs. Nonionic surfactants were selected since they are known as safe, biocompatible, and less affected by the changes in pH and ionic strength (Azeem et al. 2009). The use of co-surfactants can help to decrease the concentration of the surfactant used in the NEs.

Table 1: Composition of the prepared mucoadhesive buccal films containing atorvastatin calcium

Code of buccal films	Composition of buccal films	NE system used in the film	Components of the NE system used in the buccal films			Characterization of ATC-loaded NEs	
			Oleic acid	SCmix (Tween20: ethanol)	Distilled water	Size Z-Average (d.nm)	PDI
F1	ATC-loaded NE and HPMC (11.2 mg ATC in 2x2 cm^2)	NE 1	10%	50% (1:1)	40%	88.51 ± 0.740	0.493
F2		NE 2	10%	50% (1:2)	40%	36.75 ± 0.106	0.416
F3		NE 3	10%	50% (1:3)	40%	22.21 ± 0.402	0.437
F4		NE 4	10%	50% (1:4)	40%	17.97 ± 0.06	0.943
F0	ATC and HPMC (11.2 mg ATC in 2x2 cm^2)	-	-	-	-	-	-

Where NE: nanoemulsion, HPMC: hydroxypropyl methylcellulose, SCmix: surfactant: co-surfactant mixture, PDI: polydispersity index

Co-surfactants can decrease interfacial tension even further and improve the fluidity of the interfaces. For co-surfactants, absolute ethanol showed better solubilization of ATC than propylene glycol (Khan, Islam, and Jalil 2012) so it was chosen to be included in the NEs.

Table 2: Saturation solubility of atorvastatin calcium in different oils, surfactants, and co-surfactants

Oil, surfactant, or co-surfactant	Solubility (mg/ml)
Oleic acid	45.28 ± 1.06
Soybean oil	25.47 ± 4.10
Olive oil	8.25 ± 2.25
Sunflower oil	30.29 ± 1.36
Brij 35	33.64 ± 2.04
Tween 80	38.90 ± 3.25
Tween 20	46.68 ± 1.60
Absolute ethanol	120.66 ± 3.30
Propylene glycol	101.00 ± 3.30

Data are represented as mean ± SD (n=3).

3.2- Pseudo-ternary phase diagrams of NEs

Visual assessments of the six SCmix combinations (3:1, 2:1, 1:1, 1:2, 1:3, and 1:4 w/w) revealed that the combinations 3:1 and 2:1 were turbid and had poor flowability, hence they were excluded from any further analysis. This may be explained by increased viscosity of the system when the ratio of Tween 20 surfactant was increased.

The remaining four SCmix combinations (1:1, 1:2, 1:3, and 1:4 w/w) were used to prepare pseudo-ternary systems of oleic acid, SCmix combination and water (Figure 1). From the NEs region in the pseudo-ternary diagrams a concentration of 10% w/w of oleic acid, 50% w/w of SCmix combination, and 40% w/w of water were selected for preparation of oil/water NEs.
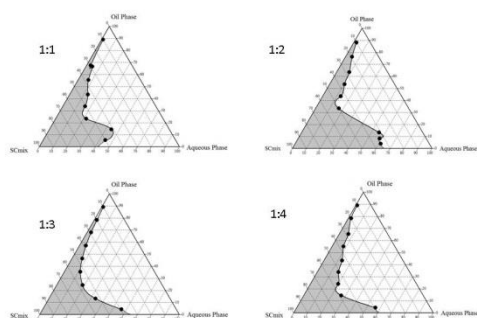
Figure 1: Pseudo-ternary phase diagrams of oleic acid, SCmix combination and water using different SCmix combinations.

3.3- Preparation and characterization of ATC-loaded NEs

Four formulations of ATC-loaded NEs (NE1, NE2, NE3 and NE4) were prepared using 10% w/w of oleic acid, 50% w/w of SCmix combination at ratios of 1:1, 1:2, 1:3, 1:4, and 40% w/w of water. The prepared NEs were subjected to further evaluation (Table 1).

3.3.1-Thermodynamic stability studies

All ATC-loaded NEs systems were physically stable during the heat, cool and freeze, thaw cycles, as well as centrifugation tests, with no phase separation creaming or cracking.

3.3.2- Droplet size analysis

The characterization of ATC-loaded NEs (Table 1) illustrated that the size of all NEs formulations were in the range of 20 to 200 nm except NE4 which showed particle size of less than 20nm, so NE4 was excluded from any further evaluation (Solans et al. 2005). The polydispersity index (PDI) of all formulations was less than one indicating narrow size distributions (Yazgan 2020). Zeta potential and the droplet size distribution of NE2 are shown in Figure 2. The low negative Zeta potential value (-0.674) can be explained by the use of nonionic surfactant in the preparation of the NE and the dilution of the NE (Salama et al. 2021). The dilution was performed by deionized water which was not expected

to affect the o/w NE, however it might have led to reduced droplet size.

3.3.3- Transmission electron microscopy

The phosphotungstic acid-stained oil droplets of NE2 were clearly apparent in Figure 2, and the droplet size corresponded well with the results of the Zetasizer droplet size analysis. Furthermore, the droplet's shape was spherical, and there was no indication of ATC precipitate in the aqueous phases. This indicates that ATC was encapsulated in an oil droplet and preferred to stay in the oil phase when water was added.
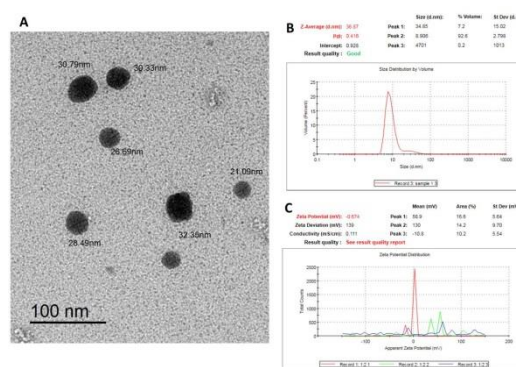
Figure 2: (A) Transmission electron micrograph of atorvastatin calcium-loaded nanoemulsion (NE2) showing size and morphology of oil droplets. (B) Particle size and particle size distribution of NE2. (C) Zeta potential of NE2.

3.4-Preparation of ATC control and NEs-based films

NEs (NE1, NE2, and NE3) were used to prepare mucoadhesive buccal films (F1, F2, and F3 respectively). According to the physical appearance of the prepared films (clarity, elasticity, and transparency), F1 showed shrinkage of size after drying and F3 had brittle sides so they were excluded from any further analysis. F2 film and the control film (F0) were further evaluated and characterized. The shrinkage of sides seen in F1 can be attributed to the highest proportion of Tween20 in the incorporated NE1 (SCmix 1:1) which increased the viscosity of the system

while the brittle sides observed with F3 may be a result of the high proportion of ethanol in NE3 (SCmix 1:3).

3.5-Spectral and thermal analyses

The FTIR spectra of ATC alone, physical mixture of ATC and HPMC, ATC-loaded NE-based film, HPMC alone, plain film, and control film are illustrated in Figure 3. The characteristic absorption spectrum of ATC in the region 3366 cm^{-1} may be due to presence of hydroxyl groups, and at the wave number 3100-3000 cm^{-1} due to the aromatic group. The above represented groups were confirmed with the standard spectrum (Lakshmi et al. 2010).
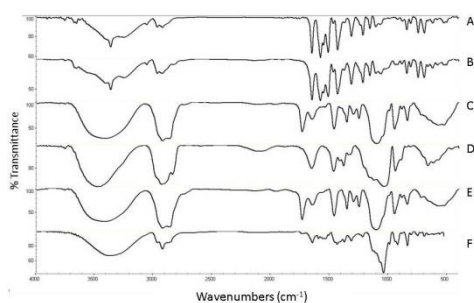
Figure 3: Fourier transform infrared spectrum of (A) atorvastatin, (B) atorvastatin + hydroxypropyl methylcellulose, (C) atorvastatin-loaded nanoemulsion-based film, (D) hydroxypropyl methylcellulose, (E) plain film (not loaded with ATC), and (F) control film (without nanaoemulsion base).

The FTIR spectrum of HPMC shows the characteristic absorption spectrum due to ether, aromatic ring, carbonyl group, C=C stretching, C-O-C stretching of aromatic ring, and C-O stretching of aromatic compound (Ramasubramaniyan et al. 2013).

The FTIR spectrum of physical mixture shows the same characteristic absorption band of the drug indicating absence of interactions between ATC and any of the film components.

Figure 4 shows a DSC thermograms of ATC alone, physical mixture of ATC and HPMC, ATC-loaded NE-based film,

HPMC alone, plain film, and control film. DSC curve of ATC show two endothermic peaks; the first appeared at 108 °C which may be related to water loss (dehydration). The second peak appeared at 154 °C representing the melting point of ATC (Dong et al. 2018).

DSC curve of HPMC alone shows water loss at three stages; at 61.86, 240.00 °C and 288.86° C. DSC thermogram of ATC and HPMC physical mixture showed peaks of HPMC and drug at their authentic location. ATC-loaded film shows the disappearance of peaks of ATC due to its solubility in the NE during the preparation of the film.
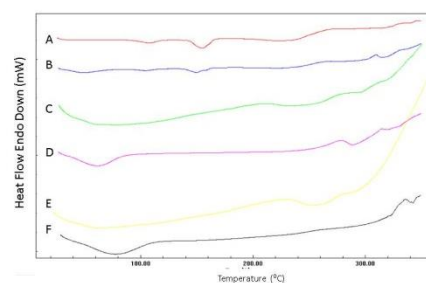
Figure 4: Differential Scanning Calorimetry thermograms of (A) atorvastatin, (B) atorvastatin + hydroxypropyl methylcellulose, (C) atorvastatin-loaded nanoemulsion-based film, (D) hydroxypropyl methylcellulose, (E) plain film (not loaded with ATC), and (F) control film (without nanaoemulsion base).

3.6- Physicochemical properties of the ATC-loaded control and NE-based mucoadhesive buccal films

The color and clarity of the formed films (control and NE-based) were visually evaluated. All of the films were transparent, had a smooth appearance, and were elastic. Table 3 shows that the physical characteristics of control film (F0) and NE-based film (F2) are nearly identical. The prepared film formulations had good thickness, weight, and drug content uniformity.

For all of the films, the weight uniformity was satisfactory according to the requirements of U. S. P XXVII, 2004. All

of the prepared control and NE-based films had average weights of 277±25 mg and 275±16 mg respectively. The drug content of the control film was determined to be between 93.0±4.9 compared to 90.0±3.2 % in the NE-based film. The drug content uniformity results showed that the drug was uniformly dispersed throughout the batches, with minimal intra-batch variability.

The folding endurance test revealed that the films had good strength and elasticity, and it was used to assess the prepared films' capacity to survive rupture. Both control and NE-based films had a folding endurance of more than 200 folds (Yellanki, and Masareddy 2011).

The control and NE-based films had moisture content of 52.4±5.8 and 44.0±3.6 %, respectively. NEs-based films showed lower moisture content than control film due to the oil content of the NEs. NEs-based films' low moisture content may aid film stability by keeping them from drying out and becoming brittle, as well as protecting them from any microbial contamination.

Swelling index of the prepared films reaches its maximum value after 30 minutes.

Following this time the swelling index tended to decrease due to start of edges' erosions (Semalty, and Nautiyal 2010).

Mucoadhesive strength was tested to ensure that the film preparations could adhere well to the buccal mucosa. The mucoadhesive properties of the tested films (Table 3) were dependent on the type and amount of the mucoadhesive polymer used. The polymer HPMC was used in the same concentration in both the control and NE-based films; therefore there was no significant variation between them. NEs served as inert carriers for drug administration.

Mucoadhesive time was approximately an hour for both control and NE-based film as mentioned before the same polymer with the same concentration was used.

Table 3: Physicochemical characteristics of the prepared films

| Physicochemical characteristics	NE-based film (F2)	Control film (F0)
Weight (mg)	277 ± 25	275 ± 16
Content uniformity (%)	93.0 ± 4.9	90.0 ± 3.2
Moisture content (%)	44.04 ± 3.6	52.36 ± 5.8
Surface pH	7.2 ± 0.09	6.81 ± 0.09
Folding endurance	> 200	> 200
Thickness (mm)	0.34 ± 1.53	0.20 ± 0.05
Swelling index	3.3 ± 0.41	4.34 ± 0.31
Mucoadhesive strength (gram) Mucoadhesive force (Dyne)	5.6 ± 0.1 5493.6 ± 98.1	4.17 ± 0.2 4090.8 ± 196.2
Mucoadhesive time (min.)	57	59

NE: nanoemulsion.

Scanning electron microscopy images of the morphology of the NE-based film and the control film are shown in Figure 5. The loaded oil of the NEs had a regular distribution and a spherical to oval shapes, as seen in Figures 5A and 5B. NEs looks to be made up of single units connected together to form a black and white-like structure at the maximum magnification used. Each unit's external surface is almost uniform and smooth, demonstrating that the surfactant creates a continuous layer around the oil droplets (Hamedi et al. 2019). On the other hand, the control film showed a smoother

Zagazig J. Pharm. Sci. Dec, 2021
Vol. 30, Issue 2, pp. 23- 40

ISSN 1110-5089
ISSN (on-line) 2356_9786

surface (Preis et al. 2014) (Figures 5C and 5D).

3.7- Ex vivo drug permeation

ATC is a medication with low-solubility (Rodde et al. 2014). To achieve sink conditions, 30% methanol was used as a solubilizer with the phosphate buffer (Alkilani et al. 2018). Figure 6 shows ex vivo permeation profile of ATC from the produced control and NE-based mucoadhesive buccal films.
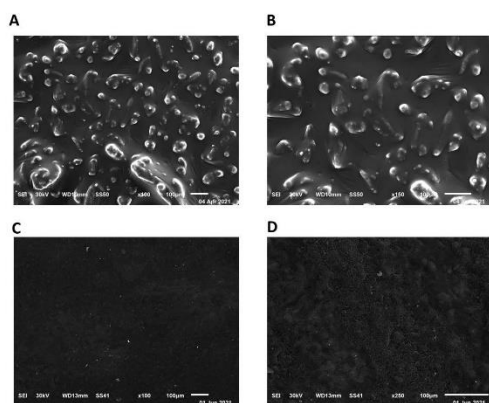

Figure 5: Scanning electron microscopy images of surface morphology of nanoemulsion-based film at x100 (A) and x150 (B) and of control film at x100 (C) and x250 (D).

The amount of ATC that permeated over the chicken pouch membrane from the NE-based film was significantly higher than the amount that permeated across the chicken pouch membrane from the control film. This might be because the NEs-based film contained penetration enhancers such oleic acid, tween 20, and ethanol. Additionally, due to the small droplet size of the ATC-loaded NE and increased drug adherence to membranes, more efficient drug transport across the chicken pouch membrane was achieved. The NEs considerably improved both hydrophilic and lipophilic drug membrane penetration. The drug in the control film was not loaded in a nano-size range so the release was lower than NE-based film.

To investigate the mechanism of drug permeation from the generated films through chicken pouch membrane, ex vivo permeation data were fitted to a variety of mathematical models, including zero-order, first-order, Higuchi, and Korsmeyer–Peppas equations. According to the r^2 values, it was evident that the best fit for control film followed zero order ($r^2 = 0.9972$) compared to first-order ($r^2 = 0.9398$) and Higuchi model ($r^2 = 0.9293$). While NE-based film followed first order release kinetics with ($r^2 = 0.9914$) compared to zero-order ($r^2 = 0.9756$) and Higuchi model ($r^2 = 0.8948$) (Koland et al. 2011). A closer look at the release for exponent value for the control and NE-based films indicated a non-Fickian (anomalous)-dominated process guided by diffusion and erosion (n=0.8829) and (n= 0.7318), respectively.
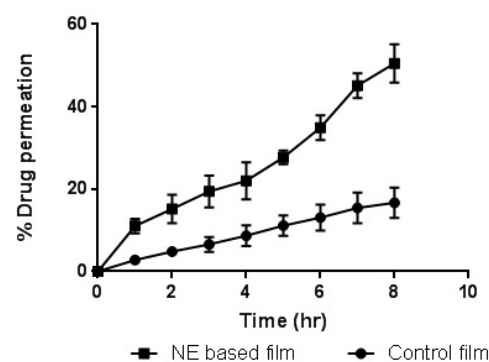
Figure 6: Ex-vivo permeation profile of atorvastatin calcium from the produced control and nanoemulsion-based mucoadhesive buccal films.
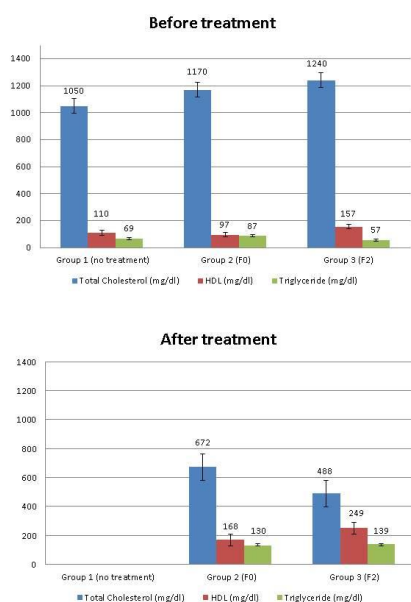
3.8-In vivo study

Rabbits are widely used in experimental protocols investigating the beneficial action of hypolipidemic drugs. Statins have been studied extensively for their anti-atherosclerotic and hypolipidemic properties (Oikonomidis et al. 2016).

After 4 weeks of cholesterol feeding, animals exhibited increased serum total cholesterol. Mean ± SD cholesterol levels were elevated from 89.33 ± 13.58 at baseline to 1153.33 ± 96.09 after induction of hyperlipidemia.

After induction of hyperlipidemia in rabbits, the first group which was sacrificed for examination of the morphologic changes that happened to the liver and heart showed great morphological changes due to cholesterol accumulation (Figures 8 and 9).

After 14 days of treatment of hyperlipedimia with F0 and F2 in the second and third group, respectively; the mean cholesterol level was significantly decreased in the two groups (P value =0.0015 and 0.0018 respectively) compared to the levels before treatments (Figure 7). On the other hand the levels of HDL (good cholesterol) levels were significantly increased in the two groups (P value=0.0019 and 0.0008 respectively). No improvements were noted in the levels of triglycerides.

Histological examination of heart and liver of sacrificed animals in the two groups showed more improved histological picture of hepatic lobules, hepatocytes, and cardiomyocytes in animals receiving NE-based film than that present in the group receiving control film (Figures 8 and 9) and these results were matched with the results obtained from blood analysis. This can be justified by the improved ATC absorption and bioavailability when loaded in nanosize in the NE (Chouksey et al. 2011).
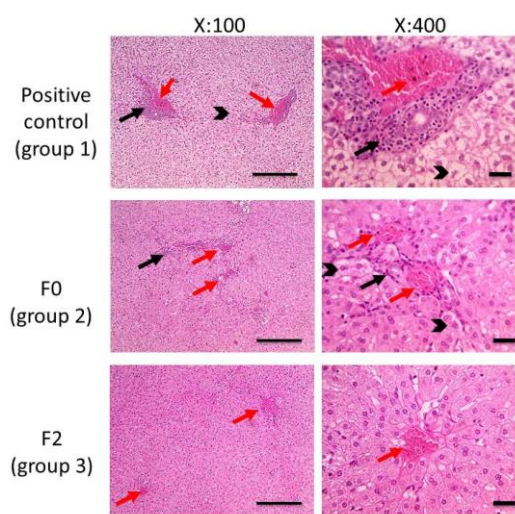
Figure 8: Microscopic pictures of H&E stained liver sections from group 1 (positive control group) are showing diffuse hydropic degeneration of hepatocytes (black arrowhead), portal congestion (red arrows) and inflammation (black arrows). Liver sections from group 2 (F0) are showing hydropic degeneration of few hepatocytes (black arrowhead), mild vascular congestion (red arrows) with few leukocytic cells infiltration (black arrows). Liver sections from group 3 (F2) are showing improved histological picture of hepatic lobules and hepatocytes, only very mild vascular congestion (red arrows) can be seen. Low magnification X: 100 bar 100, high magnification X: 400 bar 50
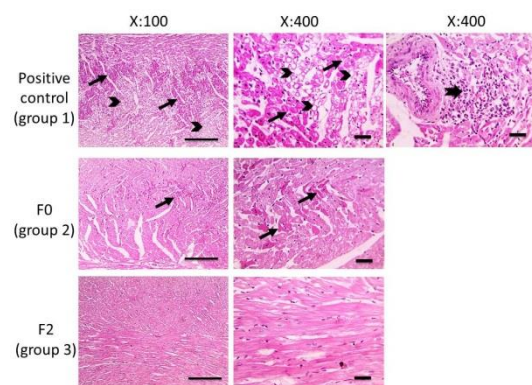

Figure 7: Levels of total cholesterol, high density lipoprotein (HDL), and triglyceride before and after receiving treatments in rabbits.

Upon comparing responses between the two groups, it was found that animals which received F2 were significantly more improved in terms of cholesterol level (P value = 0.018) and HDL levels (P = 0.007). However, there was no significant difference in triglyceride levels in the two groups.

Figure 9: Microscopic pictures of H&E stained heart sections from group 1 (positive control group) are showing marked hyalinization (thin black arrows) and macrovesicular steatosis (arrowheads) of cardiomyocytes with perivascular leukocytic cells infiltration (thick black arrow). Heart sections from group 2 (F0) are showing decreased hyalinization of cardiomyocytes (thin black arrows). Heart sections from group 3 (F2) are showing improved histological picture of cardiomyocytes. Low magnification X: 100 bar 100, high magnification X: 400 bar 50.

4. Conclusion

ATC-loaded NEs were prepared by aqueous titration method under continual vortexing. NEs-based mucoadhesive buccal films were then prepared using solvent casting technique and were successfully characterized. The current study suggests that ATC-loaded NEs-based films offered better hypolipidemic and antiatherosclerotic benefits than the control film by preventing total cholesterol levels in the blood from rising.

References

Abu-Huwaij, Rana, Rania Hamed, Enas Daoud, and Ahlam Zaid Alkilani. 2019. "Development and in Vitro Characterization of Nanoemulsion-Based Buccal Patches of Valsartan." *Acta Poloniae Pharmaceutica - Drug Research* 76(2): 313–21.

Ali, Mohammad Sajid, Mohammad Sarfaraz Alam, Nawazish Alam, and Masoom Raza Siddiqui. 2014. "Preparation, Characterization and Stability Study of Dutasteride Loaded Nanoemulsion for Treatment of Benign Prostatic Hypertrophy." *Iranian journal of pharmaceutical research: IJPR* 13(4): 1125.

Alkilani et al. 2018. "Nanoemulsion-Based Film Formulation for Transdermal Delivery of Carvedilol." *Journal of Drug Delivery Science and Technology* 46: 122–28.

Ammanage, Anand, Paul Rodriques, Amolkumar Kempwade, and Ravindra Hiremath. 2020. "Formulation and Evaluation of Buccal Films of Piroxicam Co-Crystals." *Future Journal of Pharmaceutical Sciences* 6(1): 16.

Augusthy, Ann Rose et al. 2014. "Formulation and Evaluation of Mucoadhesive Buccal Film of Lisinopril." *Res Rev J Pharm Nano* 2(1): 45–51.

Azeem, A et al. 2009. "Brief/Technical Note Nanoemulsion Components Screening and Selection: A Technical Note." *AAPS PharmSciTech* 10(1): 69–76.

Azmi, Nor Azrini Nadiha et al. 2019. "Nanoemulsions: Factory for Food, Pharmaceutical and Cosmetics." *Processes* 7(9): 617.

Chen, Lin, Caihong Wang, and Yuanchu

Wu. 2020. "Cholesterol (Blood Lipid) Lowering Potential of Rosuvastatin Chitosan Nanoparticles for Atherosclerosis: Preclinical Study in Rabbit Model." *Acta Biochimica Polonica* 67(4): 495–99.

Chouksey, Rajendra, Anand Kumar Jain, Harish Pandey, and Ankur. Maithil. 2011. "Development and Bioavailability Studies of Atorvastatin Nanoemulsion." *International Journal of Pharmacy and Life Sciences* 2(8): 982–88.

Debnath, Subhashis, Satayanarayana, and Kumar. 2011. "Nanoemulsion-A Method to Improve The Solubility of Lipophilic Drugs, Pharmanest." *Pharmanest* 2(2–3): 72–76.

Desai, Kashappa Goud H., and T. M. Pramod Kumar. 2004. "Preparation and Evaluation of a Novel Buccal Adhesive System." *AAPS PharmSciTech* 5(3).

Dong, Wenxiang et al. 2018. "Preparation, Characterization, and in Vitro/Vivo Evaluation of Polymer-Assisting Formulation of Atorvastatin Calcium Based on Solid Dispersion Technique." *Asian journal of pharmaceutical sciences* 13(6): 546–54.

El-Maghraby, Gamal M., and Mona M. Abdelzaher. 2015. "Formulation and Evaluation of Simvastatin Buccal Film." *Journal of Applied Pharmaceutical Science* 5(4): 70–77.

Giradkar, K P et al. 2010. "Design Development and in Vitro Evaluation of Bioadhesive Dosage Form for Buccal Route." *International journal of pharma*

research \& development 2: 1–24.

Hamedi, Hamid, Sara Moradi, Alan E Tonelli, and Samuel M Hudson. 2019. "Preparation and Characterization of Chitosan--Alginate Polyelectrolyte Complexes Loaded with Antibacterial Thyme Oil Nanoemulsions." *Applied Sciences* 9(18): 3933.

Hassan, Nisreen, R. K. Khar, Mushir Ali, and Javed Ali. 2009. "Development and Evaluation of Buccal Bioadhesive Tablet of an Anti-Emetic Agent Ondansetron." *AAPS PharmSciTech* 10(4): 1085–92.

Holpuch, Andrew S et al. 2012. "Evaluation of a Mucoadhesive Fenretinide Patch for Local Intraoral Delivery: A Strategy to Reintroduce Fenretinide for Oral Cancer Chemoprevention." *Carcinogenesis* 33(5): 1098–1105.

Jain, Kunal, R Suresh Kumar, Sumeet Sood, and K Gowthamarajan. 2013. "Enhanced Oral Bioavailability of Atorvastatin via Oil-in-Water Nanoemulsion Using Aqueous Titration Method." *Journal of Pharmaceutical Sciences and Research* 5(1): 18.

Jaiswal, Manjit, Rupesh Dudhe, and P K Sharma. 2015. "Nanoemulsion: An Advanced Mode of Drug Delivery System." *3 Biotech* 5(2): 123–27.

Khan, Fariba, Md Saiful Islam, and Reza-ul Jalil. 2012. "Study of Solubility of Atorvastatin Using Ternary Phase Diagram for the Development of Self-Emulsifying Drug Delivery Systems (SEDDS)." *Dhaka University*

Journal of Pharmaceutical Sciences 11(2): 83–91.

Koland, Marina, K Vijayanarayana, RNarayana Charyulu, and Prabhakara Prabhu. 2011. "In Vitro and in Vivo Evaluation of Chitosan Buccal Films of Ondansetron Hydrochloride." *International Journal of Pharmaceutical Investigation* 1(3): 164.

Kumar, A M et al. 2019. "A Review on Mucoadhesive Drug Delivery Systems." *Research Journal of Pharmaceutical Dosage Forms and Technology* 11(4): 280–87.

Lakshmi, V. et al. 2010. "Enhanced Dissolution Rate of Atorvastatin Calcium Using Solid Dispersion with PEG 6000 by Dropping Method." *Journal of Pharmaceutical Sciences and Research* 2(8): 484–91.

Lennernäs, Hans. 2003. "Clinical Pharmacokinetics of Atorvastatin." *Clinical pharmacokinetics* 42(13): 1141–60.

Mohamed, Magdy I., Mohamed Haider, and Muaadh A.Mohamed Ali. 2011. "Buccal Mucoadhesive Films Containing Antihypertensive Drug: In Vitro/in Vivo Evaluation." *Journal of Chemical and Pharmaceutical Research* 3(6): 665–86.

Nair, Anroop B. et al. 2020. "Mucoadhesive Buccal Film of Almotriptan Improved Therapeutic Delivery in Rabbit Model." *Saudi Pharmaceutical Journal* 28(2): 201–9.

Oikonomidis, Nikolaos et al. 2016. "Pre-Treatment with Simvastatin Prevents the Induction of Diet-Induced Atherosclerosis in a Rabbit Model." *Biomedical Reports* 5(6): 667–74.

Pendekal, Mohamed S, and Pramod K Tegginamat. 2012. "Formulation and Evaluation of a Bioadhesive Patch for Buccal Delivery of Tizanidine." *Acta Pharmaceutica Sinica B* 2(3): 318–24.

Poli, Andrea. 2007. "Atorvastatin." *Drugs* 67(1): 3–15.

Preis, Maren et al. 2014. "Design and Evaluation of Bilayered Buccal Film Preparations for Local Administration of Lidocaine Hydrochloride." *European Journal of Pharmaceutics and Biopharmaceutics* 86(3): 552–61.

Ramadan, E., Th Borg, G. M. Abdelghani, and N. M. Saleh. 2013. "Formulation and Evaluation of Acyclovir Microemulsions." *Bulletin of Pharmaceutical Sciences* 36(March): 31–47.

Ramasubramaniyan, P, S Palanichamy, V M Deepu, and M Rajesh. 2013. "Formulation and Evaluation of Amlodipine Besylate Floating Tablets." *Res J Phar Biol Chem Sci* 4(4): 15–33.

Rashid, Shirya, Kristine D Uffelman, P Hugh R Barrett, and Gary F Lewis. 2002. "Effect of Atorvastatin on High-Density Lipoprotein Apolipoprotein AI Production and Clearance in the New Zealand White Rabbit." *Circulation* 106(23): 2955–60.

Rodde, Madhuri S., Ganesh T. Divase, Tejas B. Devkar, and Avinash R. Tekade. 2014. "Solubility and Bioavailability Enhancement of Poorly Aqueous Soluble

Atorvastatin: In Vitro, Ex Vivo, and in Vivo Studies." *BioMed Research International* 2014.

Salama AH, Basha M, Salama AAA. 2021. Micellar buccal film for safe and effective control of seizures: Preparation, in vitro characterization, ex vivo permeation studies and in vivo assessment. Eur J Pharm Sci Off J Eur Fed Pharm Sci. 166:105978.

Salehi, Sahar, and Soheil Boddohi. 2017. "New Formulation and Approach for Mucoadhesive Buccal Film of Rizatriptan Benzoate." *Progress in Biomaterials* 6(4): 175–87.

Semalty, A., Mona Semalty, and U. Nautiyal. 2010. "Formulation and Evaluation of Mucoadhesive Buccal Films of Enalapril Maleate." *Indian Journal of Pharmaceutical Sciences* 72(5): 571–75.

Shafiq, Sheikh et al. 2007. "Development and Bioavailability Assessment of Ramipril Nanoemulsion Formulation." *European journal of pharmaceutics and biopharmaceutics* 66(2): 227–43.

Shailaja, T et al. 2012. "A Novel Bioadhesive Polymer: Grafting of Tamarind Seed Polysaccharide and Evaluation of Its Use in Buccal Delivery of Metoprolol

Succinate." *Der Pharmacia Lettre* 4(2): 487–508.

Singh, S. et al. 2008. "Preparation and Evaluation of Buccal Bioadhesive Films Containing Clotrimazole." *AAPS PharmSciTech* 9(2): 660–67.

Solans, C. et al. 2005. "Nano-Emulsions." *Current Opinion in Colloid and Interface Science* 10(3–4): 102–10.

Sumbul, S, and S I Ahmed. 2012. "Anti-Hyperlipidemic Activity of Carissa Carandas (Auct.) Leaves Extract in Egg Yolk Induced Hyperlipidemic Rats." *J Basic Appl Sci* 8: 124–34.

Yazgan, Hatice. 2020. "Investigation of Antimicrobial Properties of Sage Essential Oil and Its Nanoemulsion as Antimicrobial Agent." *LWT* 130: 109669.

Yellanki, S. K., S. Jagtap, and R. Masareddy. 2011. "Dissofilm: A Novel Approach for Delivery of Phenobarbital; Design and Characterization." *Journal of Young Pharmacists* 3(3): 181–88.

Yen, Ching Chi et al. 2018. "Nanoemulsion as a Strategy for Improving the Oral Bioavailability and Anti-Inflammatory Activity of Andrographolide." *International Journal of Nanomedicine* 13: 669–80.

تطوير وتوصيف الأفلام الشدقية القائمة على مستحلب النانو لأتورفاستاتين كالسيوم لتعزيز التأثير على انقاص شحميات الدم

فاطمة بكر1, معتزه محمود سليمان2, حسن محمد الصباغ1

_____

1 قسم الصيدلانيات, كلية الصيدلة, جامعة المنصورة, جمهورية مصر العربية.

2 قسم الصيدلة الاكلينيكية والممارسة الصيدلية, كلية الصيدلة, جامعة المنصورة, جمهورية مصر العربية.

الملخص

الأهداف: يستخدم أتورفاستاتين كالسيوم على نطاق واسع لعلاج فرط شحميات الدم ولكن فعاليته محدودة بسبب قلة إتاحته الحيوية عن طريق الفم. كان الهدف من هذه الدراسة هو صياغة وتقييم أفلام اللصق المخاطي التي تحتوي على مستحلب نانوي محمّل بـأتورفاستاتين في محاولة لتعزيز فعالية أتورفاستاتين لتقليل شحميات الدم.

الطرق: بناءً على معلومات مختلفة ، بما في ذلك قابلية أتورفاستاتين للذوبان ، ومتوسط حجم القطرة في المستحلب النانوي ، والوضوح ، والاستقرار الديناميكي الحراري ، وقابلية التدفق ، تم اختيار مكونات المستحلب النانوي المثلى التي تضمنت 10٪ حمض الأوليك كزيت ، و 50٪ توين 20: إيثانول بنسب مختلفة كخليط خافض للتوتر السطحي و 40٪ ماء. تم تحضير أفلام اللصق المخاطي باستخدام هيدروكسي بروبيل ميثيل سليلوز ممزوجًا مع المستحلب النانوي المُحمل بأتورفاستاتين بواسطة تقنية صب المذيبات. تم إخضاع الأفلام المحضرة إلى تقييمات مختلفة بما في ذلك الخصائص الفيزيائية والكيميائية ، وخصائص الالتصاق للأغشية المخاطية ، وإطلاق الدواء خارج الجسم الحي ، وأخيراً خضعت لدراسة في الجسم الحي لتقييم الفعالية في علاج الأرانب المصابة بفرط كوليسترول الدم الناجم عن النظام الغذائي.

النتائج: أظهر الفيلم اللاصق المخاطي المحتوي على المستحلب النانوي والفيلم المرجعي خصائص فيزيائية مقبولة دون اختلاف كبير في خصائص الالتصاق الي الاغشية المخاطية. كان الفيلم المحتوي على المستحلب النانوي أكثر فاعلية في تعزيز تغلغل الدواء خلال الغشاء المخاطي المستخرج من كيس الدجاج. كشفت الدراسة في الجسم الحي أن كلا من تحليل الدم والفحص التشريحي أثبتا الفعالية الفائقة للفيلم المحتوي على المستحلب النانوي في خفض مستوى الكوليسترول في الأرانب المصابة بفرط كوليسترول الدم مقارنة بالفيلم المرجعي.

الاستنتاج: نجحت أفلام اللصق المخاطي المحتوية على المستحلب النانوي المحمل بأتورفاستاتين في تعزيز فوائد أتورفاستاتين في انقاص شحميات الدم ، في الأرانب المختبرة ، مقارنة بالفيلم المرجعي وذلك من خلال تحسين قابلية الذوبان والاتاحة الحيوية للعقار.